Annals of Mathematics and Computer Science ISSN: 2789-7206
Vol 37 (2026) 1-14 https://doi.org/10.56947/amcs.v37.965

ADOMIAN–ELZAKI METHOD FOR FRACTIONAL KDV EQUATIONS

MADHUKAR POPATRAO ZANJE[1*] AND SHANTARAM NARAYAN SALUNKHE[2]

Abstract. We revisit the Adomian–Elzaki transform method for the time-fractional Korteweg–de Vries equation with a Caputo derivative of order α between 0 and 1. For initial data that are linear in the space variable, we prove that the underlying operator is a strict contraction on an explicit Banach space and that the Adomian terms are bounded by Catalan numbers. This gives a computable a priori error bound for every α. For soliton initial data, the series converges for times below π when α equals 1, whereas numerical evidence shows divergence for every smaller α. The arithmetic complexity is also analysed.

Keywords. Caputo derivative, Elzaki transform, Adomian decomposition, fractional KdV equation, convergence analysis.
2020 Mathematics Subject Classification. Primary 35R11; Secondary 35Q53, 65M12.

1. Introduction

The Korteweg–de Vries (KdV) equation $u_t + 6uu_x + u_{xxx} = 0$ is a fundamental model for weakly nonlinear dispersive waves, such as long waves in shallow water, and it admits the classical solitary-wave solution [8]. Replacing u_t by a Caputo derivative of order $0 < \alpha \leq 1$ gives the time-fractional KdV equation

$$ {}^{C}D_t^{\alpha} u + 6uu_x + u_{xxx} = 0, \qquad u(x,0) = f(x), \tag{1.1}$$

which describes dispersive waves in media with memory: the Caputo derivative replaces the instantaneous rate of change by a weighted average over the whole past [2, 4]. Fractional derivatives of Caputo type and their generalizations, such as the proportional Caputo derivative, continue to be studied intensively; see, for example, the recent analysis of chaotic behaviour of a proportional Caputo derivative in this journal [11].

Semi-analytical series methods are widely used for (1.1). The Adomian decomposition method [1], whose convergence under contraction-type conditions was studied by Cherruault [3], was applied to the fractional KdV equation by Momani [10], and combinations of the Elzaki transform [6] with iterative schemes have

Date: Received: Sep 13, 2026; Revised: Oct 12, 2026; Accepted: Oct 19, 2026.
* Corresponding author
© The Author(s) 2026. This article is licensed under a Creative Commons Attribution-NonCommercial-NoDerivatives 4.0 International License. To view a copy of the licence, visit https://creativecommons.org/licenses/by-nc-nd/4.0/.

been applied to fractional KdV systems [7]. Related transform–decomposition and transform–iteration methods have recently been analysed in this journal: Oyefusi et al. [12] showed that a coupled transform–Adomian method is equivalent to a Picard iteration and proved convergence under a contraction condition, and Zair et al. [13] analysed a Laplace variational iteration method for fractional Burgers equations.

For the KdV equation, however, a contraction condition cannot simply be assumed. The term u_{xxx} removes three orders of spatial smoothness at each step, while the fractional integral restores none of them, so the integral operator associated with (1.1) does not map any fixed space of finitely differentiable functions into itself. It is classical that formal power series in t for equations whose spatial order exceeds their temporal order may diverge even for analytic data [9]. The convergence of the Adomian series for (1.1) must therefore be established for specific classes of data, and it may genuinely fail.

The contribution of this paper is to settle this question for two standard classes of initial data. For data that are linear in x, we identify an explicit Banach space on which the Adomian–Elzaki operator is a strict contraction, with a contraction constant given explicitly in terms of α, the time horizon and the initial data. We also show that the Adomian components themselves are bounded by Catalan numbers, which yields a computable a priori error bound that we compare with observed errors. For soliton data, we prove convergence for $t < \pi$ when $\alpha = 1$, identify in closed form the term that destroys this convergence when $\alpha < 1$, and give numerical and residual-based evidence that the series then diverges for every $t > 0$. Finally, we analyse the arithmetic cost of generating the Adomian polynomials and compare it with measured computing times.

The paper is organized as follows. Section 2 collects the properties of fractional operators, the Elzaki transform, Adomian polynomials and Catalan numbers that are used later. Section 3 derives the Adomian–Elzaki recursion and gives the first components explicitly for both classes of data. Section 4 contains the convergence analysis, Section 5 the numerical results, and Section 6 a discussion of their implications. Section 7 concludes.

2. Preliminaries

2.1. **Fractional integrals and derivatives.** The Gamma function $\Gamma(z) = \int_0^\infty s^{z-1}e^{-s}\,ds$ is logarithmically convex on $(0,\infty)$ by the Bohr–Mollerup theorem. Hence $\varphi(x) = \ln\Gamma(1+x)$ is convex on $[0,\infty)$ with $\varphi(0) = 0$, and convexity gives $\varphi(x) \le \frac{x}{x+y}\varphi(x+y)$ and $\varphi(y) \le \frac{y}{x+y}\varphi(x+y)$ for $x, y \ge 0$ with $x + y > 0$. Adding these two inequalities yields the superadditivity property

$$\Gamma(x+y+1) \ge \Gamma(x+1)\,\Gamma(y+1), \qquad x, y \ge 0, \tag{2.1}$$

which will be used in Section 4.

For $\alpha > 0$ the Riemann–Liouville integral and, for $0 < \alpha < 1$, the Caputo derivative of a function g on $[0, T]$ are

$$I_t^\alpha g(t) = \frac{1}{\Gamma(\alpha)} \int_0^t (t-s)^{\alpha-1} g(s)\, ds, \qquad {}^C D_t^\alpha g(t) = \frac{1}{\Gamma(1-\alpha)} \int_0^t (t-s)^{-\alpha} g'(s)\, ds, \tag{2.2}$$

with ${}^C D_t^\alpha g = g'$ for $\alpha = 1$ [2, 4]. Thus ${}^C D_t^\alpha g = I_t^{1-\alpha} g'$. The following properties are standard [4]. The integrals form a semigroup, $I_t^\alpha I_t^\beta = I_t^{\alpha+\beta}$, and act on powers by

$$I_t^\alpha \Big[\frac{t^\beta}{\Gamma(\beta+1)}\Big] = \frac{t^{\beta+\alpha}}{\Gamma(\beta+\alpha+1)} \quad (\beta > -1), \qquad {}^C D_t^\alpha \Big[\frac{t^\beta}{\Gamma(\beta+1)}\Big] = \frac{t^{\beta-\alpha}}{\Gamma(\beta-\alpha+1)} \quad (\beta > 0), \tag{2.3}$$

while ${}^C D_t^\alpha 1 = 0$. For absolutely continuous g, the fundamental relation $I_t^\alpha {}^C D_t^\alpha g(t) = g(t) - g(0)$ holds, and for continuous g the elementary estimate

$$\|I_t^\alpha g\|_{\infty,[0,T]} \le \frac{T^\alpha}{\Gamma(\alpha+1)} \|g\|_{\infty,[0,T]} \tag{2.4}$$

follows from $I_t^\alpha 1 = t^\alpha/\Gamma(\alpha+1)$. Estimate (2.4) is the only property of the fractional integral needed in the contraction argument.

2.2. **The Elzaki transform.** For a function g of exponential order on $[0, \infty)$, the Elzaki transform is [6]

$$\mathcal{E}[g](v) = v \int_0^\infty e^{-t/v} g(t)\, dt. \tag{2.5}$$

If $G(p)$ denotes the Laplace transform of g, then $\mathcal{E}[g](v) = v\, G(1/v)$, so every property of the Laplace transform has an Elzaki counterpart. In particular, for $\beta > -1$ and real a,

$$\mathcal{E}[t^\beta] = \Gamma(\beta+1)\, v^{\beta+2}, \qquad \mathcal{E}[e^{at}] = \frac{v^2}{1-av}, \qquad \mathcal{E}[\sin at] = \frac{av^3}{1+a^2v^2}, \qquad \mathcal{E}[\cos at] = \frac{v^2}{1+a^2v^2}, \tag{2.6}$$

where the second formula requires $av < 1$. Integration by parts gives $\mathcal{E}[g'](v) = \mathcal{E}[g](v)/v - v\, g(0)$. For the convolution $(g * h)(t) = \int_0^t g(t-s)h(s)\, ds$, the Laplace convolution theorem gives

$$\mathcal{E}[g * h](v) = v\, G(1/v)\, H(1/v) = \frac{1}{v}\, \mathcal{E}[g](v)\, \mathcal{E}[h](v). \tag{2.7}$$

Since $I_t^\alpha g = k_\alpha * g$ with $k_\alpha(t) = t^{\alpha-1}/\Gamma(\alpha)$, and $\mathcal{E}[k_\alpha] = v^{\alpha+1}$ by (2.6), formula (2.7) yields

$$\mathcal{E}[I_t^\alpha g](v) = v^\alpha\, \mathcal{E}[g](v), \qquad \text{equivalently} \qquad \mathcal{E}^{-1}\big[v^\alpha \mathcal{E}[g](v)\big] = I_t^\alpha g(t). \tag{2.8}$$

Combining (2.8), with α replaced by $1-\alpha$, with the rule for $\mathcal{E}[g']$, we obtain the Elzaki transform of the Caputo derivative,

$$\mathcal{E}[{}^C D_t^\alpha g](v) = v^{1-\alpha}\Big(\frac{\mathcal{E}[g](v)}{v} - v\, g(0)\Big) = v^{-\alpha}\mathcal{E}[g](v) - v^{2-\alpha} g(0). \tag{2.9}$$

Formulas (2.8) and (2.9) are the only properties of the transform used to derive the method.

2.3. **Adomian polynomials.** For a nonlinear operator N and a series $u = \sum_{n\geq 0} u_n$, the Adomian polynomials are [1]

$$A_n = \frac{1}{n!}\frac{d^n}{d\lambda^n} N\Big(\sum_{j\geq 0} \lambda^j u_j\Big)\Big|_{\lambda=0}, \qquad n \geq 0, \tag{2.10}$$

so that formally $N(u) = \sum_{n\geq 0} A_n$, with A_n depending only on $u_0, \ldots, u_n$. For the KdV nonlinearity $N(u) = uu_x$, the expression inside (2.10) is a product of two power series in λ, and A_n is the coefficient of λ^n in their Cauchy product:

$$A_n = \sum_{j=0}^{n} u_j\,(u_{n-j})_x, \tag{2.11}$$

that is, $A_0 = u_0u_{0,x}$, $A_1 = u_0u_{1,x} + u_1u_{0,x}$, $A_2 = u_0u_{2,x} + u_1u_{1,x} + u_2u_{0,x}$ and $A_3 = u_0u_{3,x} + u_1u_{2,x} + u_2u_{1,x} + u_3u_{0,x}$. The Cauchy-product structure also shows that, whenever $\sum u_n$ and $\sum (u_n)_x$ converge absolutely, $\sum_n A_n = \big(\sum_n u_n\big)\big(\sum_n u_n\big)_x$.

2.4. **Catalan numbers.** The Catalan numbers $C_n = \binom{2n}{n}/(n+1)$, that is $1, 1, 2, 5, 14, 42, \ldots$, satisfy the recursion $C_0 = 1$, $C_{n+1} = \sum_{j=0}^{n} C_jC_{n-j}$. Their generating function is

$$\sum_{n\geq 0} C_n z^n = \frac{1 - \sqrt{1-4z}}{2z}, \qquad |z| \leq \tfrac{1}{4}, \tag{2.12}$$

which equals 2 at $z = 1/4$. Moreover $C_n \leq 4^n$ and $C_n \sim 4^n/(\sqrt{\pi}\, n^{3/2})$ as $n \to \infty$. The recursion for C_n has the same form as the Cauchy-product recursion (2.11), which is why Catalan numbers appear in the bounds of Section 4.

3. The Adomian–Elzaki recursion

Applying the Elzaki transform to (1.1) and using (2.9) gives $v^{-\alpha}\mathcal{E}[u] - v^{2-\alpha} f = -\mathcal{E}[u_{xxx} + 6uu_x]$. Multiplying by v^α, and using $\mathcal{E}[f] = v^2 f$ and (2.8), we obtain the equivalent integral equation

$$u = \mathcal{T}(u) := f - I_t^\alpha\big[u_{xxx} + 6uu_x\big]. \tag{3.1}$$

Writing $u = \sum_{n\geq 0} u_n$ and expanding uu_x in the Adomian polynomials (2.11), we obtain the Adomian–Elzaki recursion

$$u_0 = f, \qquad u_{n+1} = -I_t^\alpha\Big[(u_n)_{xxx} + 6\sum_{j=0}^{n} u_j\,(u_{n-j})_x\Big] \quad (n \geq 0), \tag{3.2}$$

and $\phi_N = \sum_{n=0}^{N-1} u_n$ denotes the N-term approximation. In practice the method consists of four steps: the initial function is taken as u_0; at step n the Adomian polynomial A_n is formed from $u_0, \ldots, u_n$ by (2.11); the integral I_t^α is applied to $(u_n)_{xxx} + 6A_n$, which by (2.8) is the same as multiplying its Elzaki transform by v^α and inverting; and the partial sum is updated. The step count N is either fixed in advance or chosen by monitoring the residual defined in Section 5.

If f is independent of t, an induction based on (2.3) shows that every component has the separated form

$$u_n(x,t) = \frac{t^{n\alpha}}{\Gamma(n\alpha+1)}\,P_n(x), \qquad P_{n+1} = -\Big[P_n''' + 6\sum_{j=0}^{n} B_\alpha(j,n-j)\,P_j\,P_{n-j}'\Big], \tag{3.3}$$

with $P_0 = f$ and $B_\alpha(j,k) = \Gamma((j+k)\alpha+1)/\big(\Gamma(j\alpha+1)\Gamma(k\alpha+1)\big)$. Indeed, the product of the time factors of u_j and u_k equals $B_\alpha(j,k)\,t^{(j+k)\alpha}/\Gamma((j+k)\alpha+1)$, and the first identity in (2.3) raises the index by one. For $\alpha = 1$ the coefficients $B_1(j,k) = \binom{j+k}{j}$ are binomial; for $\alpha < 1$ they are not, and by (2.1) they satisfy $B_\alpha(j,k) \geq 1$. The only coefficient entering the first three components that differs from its value at $\alpha = 1$ is

$$\beta_2 := B_\alpha(1,1) = \frac{\Gamma(2\alpha+1)}{\Gamma(\alpha+1)^2}, \tag{3.4}$$

which increases from 1 to 2 as α increases from 0 to 1 (for example, $\beta_2 = 1.574$ for $\alpha = 0.75$ and $\beta_2 = 1.273$ for $\alpha = 0.5$). All numerical results below are computed from (3.3).

3.1. **Explicit components for linear data.** For $f(x) = cx$, all components are linear in x, and (3.3) gives

$$u_0 = cx, \quad u_1 = -\frac{6c^2t^\alpha}{\Gamma(\alpha+1)}\,x, \quad u_2 = \frac{72c^3t^{2\alpha}}{\Gamma(2\alpha+1)}\,x, \quad u_3 = -\frac{216c^4(4+\beta_2)\,t^{3\alpha}}{\Gamma(3\alpha+1)}\,x. \tag{3.5}$$

For $\alpha = 1$ these reduce to $u_n = c(-6ct)^n x$, the expansion of the exact solution $u = cx/(1+6ct)$.

3.2. **Explicit components for soliton data.** For $f(x) = \frac{1}{2}\operatorname{sech}^2(x/2)$, write $s = \operatorname{sech}(x/2)$ and $\tau = \tanh(x/2)$, so that $s' = -\frac{1}{2}s\tau$ and $\tau' = \frac{1}{2}s^2$. Every P_n is then a polynomial in τ of degree $3n+2$, and (3.3) gives

$$\begin{aligned} u_1 &= \frac{t^\alpha}{\Gamma(\alpha+1)}\,\frac{s^2\tau}{2}, \qquad u_2 = \frac{t^{2\alpha}}{\Gamma(2\alpha+1)}\,\frac{s^2(2-3s^2)}{4}, \\ u_3 &= \frac{t^{3\alpha}}{\Gamma(3\alpha+1)}\Big[-\frac{s^2\tau(3s^2-1)}{2} + \frac{3}{4}\,(2-\beta_2)\,s^4\tau(3s^2-2)\Big]. \end{aligned} \tag{3.6}$$

For $\alpha = 1$ we have $\beta_2 = 2$, the second term in u_3 vanishes, and $P_n = (-1)^n f^{(n)}$, in agreement with the Taylor expansion of the travelling wave $U(x,t) = f(x-t)$. For $\alpha < 1$, however, $\beta_2 < 2$ and the additional term $\frac{3}{4}(2-\beta_2)s^4\tau(3s^2-2)$ appears. It is the first instance of the loss of cancellation that is analysed in Section 4: at $\alpha = 1$ the three spatial derivatives produced by u_{xxx} at each step are compensated by the nonlinear term, so that P_n contains only n derivatives of f, whereas for $\alpha < 1$ the compensation is incomplete and the number of derivatives grows by three at each step.

4. Convergence analysis

4.1. **Initial data linear in space.** Let $f(x) = cx$ with $c > 0$, let $\Omega = [-\ell, \ell]$ and $T > 0$, and consider

$$X_T = \{u(x,t) = a(t)\,x : \ a \in C[0,T]\}, \qquad \|u\|_X = \max_{\Omega\times[0,T]} |u| = \ell\,\|a\|_\infty.$$

As a closed subspace of $C(\Omega \times [0,T])$, X_T is a Banach space. For $u = a(t)x \in X_T$ we have $u_{xxx} = 0$ and $uu_x = a^2 x$, so $\mathcal{T}(u) = \big(c - 6I_t^\alpha[a^2]\big)x$ and $\mathcal{T}$ maps X_T into itself. Let $B = \{a(t)x \in X_T : \ \|a\|_\infty \le 2c\}$ and define

$$L = \frac{24\,c\,T^\alpha}{\Gamma(\alpha+1)} = \frac{24\,\|f\|_{\infty,\Omega}\,T^\alpha}{\ell\,\Gamma(\alpha+1)}. \tag{4.1}$$

We now show that, if $L < 1$, then $\mathcal{T}$ is a strict contraction on B with constant L, so that (1.1) has a unique solution in B. By (2.4), for a, b with $\|a\|_\infty, \|b\|_\infty \le 2c$ we obtain $\|c - 6I_t^\alpha[a^2]\|_\infty \le c + 24c^2T^\alpha/\Gamma(\alpha+1) = c(1+L) \le 2c$, so $\mathcal{T}(B) \subseteq B$, and

$$\|\mathcal{T}(ax) - \mathcal{T}(bx)\|_X = 6\ell\,\big\|I_t^\alpha[(a+b)(a-b)]\big\|_\infty \le \frac{24c\,T^\alpha}{\Gamma(\alpha+1)}\,\ell\|a-b\|_\infty = L\,\|ax-bx\|_X.$$

Banach's fixed-point theorem now gives the claim. The constant L depends on the fractional order through $T^\alpha/\Gamma(\alpha+1)$, on the initial data through $c = \|f\|_{\infty,\Omega}/\ell$, and on the domain only through this ratio, because the problem is invariant under the scaling $x \mapsto \ell x$. The condition $L < 1$ is equivalent to the explicit time horizon

$$T < T^*(\alpha) = \Big(\frac{\Gamma(\alpha+1)}{24\,c}\Big)^{1/\alpha}. \tag{4.2}$$

4.2. **Bounds for the Adomian terms.** The contraction property concerns the Picard iterates; we now show that the Adomian components themselves satisfy a geometric bound with the same constant. For $f = cx$, (3.3) gives $u_n = a_n(t)\,x$ with $a_n(t) = c(-6c)^n\gamma_n t^{n\alpha}$, where $\gamma_0 = 1$ and

$$\gamma_{n+1} = \frac{\Gamma(n\alpha+1)}{\Gamma((n+1)\alpha+1)}\sum_{j=0}^{n}\gamma_j\gamma_{n-j}. \tag{4.3}$$

By the superadditivity property (2.1), $\Gamma((n+1)\alpha+1) \ge \Gamma(n\alpha+1)\Gamma(\alpha+1)$. Comparing (4.3) with the recursion $C_{n+1} = \sum_{j=0}^{n} C_jC_{n-j}$ of the Catalan numbers, induction gives $\gamma_n \le C_n/\Gamma(\alpha+1)^n$. With $\lambda = L/4$ and $C_n \le 4^n$ we therefore obtain, on $\Omega \times [0,T]$,

$$\|u_n\|_X \le \ell\,c\,C_n\,\lambda^n \le \ell\,c\,L^n. \tag{4.4}$$

Hence, for $L < 1$ the Adomian series converges absolutely in X_T. By the Cauchy product of absolutely convergent series, $\sum_n A_n = \big(\sum_n u_n\big)\big(\sum_n u_n\big)_x$, so summing (3.2) shows that the sum is a fixed point of $\mathcal{T}$. The sum lies in B, because the generating function of the Catalan numbers (2.12) gives $\sum_n C_n\lambda^n \le 2$ for $\lambda \le 1/4$, and it therefore coincides with the unique solution in B. Summing the tail of (4.4) yields the computable a priori truncation bound

$$\|u - \phi_N\|_X \le \ell\,c\sum_{n\ge N} C_n\lambda^n \le \frac{\ell\,c\,L^N}{1-L}. \tag{4.5}$$

4.3. **Soliton data.** For $f(x) = \frac{1}{2}\operatorname{sech}^2(x/2)$ and $\alpha = 1$, the exact solution is $U(x,t) = \frac{1}{2}\operatorname{sech}^2((x-t)/2)$. For $\alpha = 1$ we have $B_1(j,k) = \binom{j+k}{j}$, and (3.3) becomes the Leibniz rule for ∂_t^n applied to $u_t = -6uu_x - u_{xxx}$. Hence $u_n = t^n\,\partial_t^n U(x,0)/n!$, and ϕ_N is the Taylor polynomial of U in t. The function $U(x,\cdot)$ has poles at $t = x \pm i\pi(2k+1)$, so for every real x it is analytic in the disc $|t| < \pi$, and the radius π is attained at $x = 0$. For $|t| \le r < \pi$ and $w = (x-t)/2$, we have $|\cosh w|^2 = \sinh^2(\operatorname{Re} w) + \cos^2(\operatorname{Im} w) \ge \cos^2(r/2)$, so $|U| \le \frac{1}{2}\sec^2(r/2)$. The Cauchy estimates then give, uniformly in $x \in \mathbb{R}$ and for $0 \le t \le T < r < \pi$,

$$|U(x,t) - \phi_N(x,t)| \le \frac{\sec^2(r/2)}{2}\,\frac{(T/r)^N}{1 - T/r}. \tag{4.6}$$

For $\alpha < 1$, the coefficients $B_\alpha(j,k)$ are no longer binomial, and the cancellation that reduces the three spatial derivatives of u_{xxx} to a single time derivative at each step is lost; the first trace of this is the term proportional to $2 - \beta_2$ in (3.6). Our computations (Section 5) show that $\|P_n\|_\infty/\Gamma(n\alpha+1)$ then grows faster than any geometric sequence, so that the Adomian–Elzaki series diverges for every $t > 0$. This is the behaviour expected from [9] for equations whose spatial order exceeds their temporal order. Consequently, no contraction estimate of the form $\|u_{n+1}\| \le L\|u_n\|$ can hold for this data when $\alpha < 1$, and the partial sums ϕ_N can at best be used as an asymptotic approximation for small t and small N.

5. Numerical results

All values below were computed from (3.3) in Python with double precision; the soliton components for $\alpha = 1$ were computed in exact rational arithmetic, with polynomials in $\tanh(x/2)$.

5.1. **Linear initial data.** We take $c = 1/6$, so that for $\alpha = 1$ the exact solution is $u = x/(6(1+t))$, and $\ell = 1$. A reference solution is obtained by summing 400 terms, which is admissible because all test times satisfy $L \le 1/2$. It agrees with an independent implicit product-trapezoidal time-marching solution [5] to within 1.5×10^{-9}. For each α we choose the times at which $L = 1/4$ and $L = 1/2$, and Table 1 compares the observed maximum error on $\Omega \times [0,t]$ with the Catalan bound and the geometric bound of (4.5). Both bounds hold in every case. The Catalan bound is sharper by one to two orders of magnitude, and the observed errors are smaller still, because $C_n 4^{-n} \sim n^{-3/2}/\sqrt{\pi}$ and because the bound $\Gamma((n+1)\alpha+1) \ge \Gamma(n\alpha+1)\Gamma(\alpha+1)$ is not sharp. Figure 1 shows the coefficient $a(t)$ and the error decay for $\alpha = 0.75$. For comparison, the numerically estimated radius of convergence of the series in t is 1, 0.81, 0.55 and 0.18 for $\alpha = 1$, 0.9, 0.75 and 0.5, whereas (4.2) guarantees 0.25, 0.21, 0.14 and 0.05.

5.2. **Soliton initial data.** Table 2 compares the maximum error of ϕ_N on $[-20,20] \times [0,T]$ for $\alpha = 1$ with the bound (4.6), minimised over $r \in (T,\pi)$. The bound holds throughout and, for $T \le 1$, exceeds the observed error by only about one order of magnitude. Figure 3 shows the ten-term approximation for $\alpha = 1$, and Figure 2 shows it as a surface together with its error, which grows with t as predicted by (4.6) and reaches 2.4×10^{-3} at $t = 1.5$.

TABLE 1. Linear initial data ($c = 1/6$, $\ell = 1$): observed maximum error of ϕ_N and the a priori bounds (4.5).

α	t	L	N	observed	Catalan bound	geometric bound
1.00	0.0625	0.25	5	1.50×10^{-7}	8.32×10^{-6}	2.17×10^{-4}
1.00	0.0625	0.25	10	1.43×10^{-13}	3.26×10^{-9}	2.12×10^{-7}
1.00	0.1250	0.50	5	4.52×10^{-6}	3.57×10^{-4}	1.04×10^{-2}
1.00	0.1250	0.50	10	1.38×10^{-10}	4.66×10^{-6}	3.26×10^{-4}
0.90	0.0440	0.25	5	2.37×10^{-7}	8.32×10^{-6}	2.17×10^{-4}
0.90	0.0440	0.25	10	4.49×10^{-13}	3.26×10^{-9}	2.12×10^{-7}
0.90	0.0950	0.50	5	7.12×10^{-6}	3.57×10^{-4}	1.04×10^{-2}
0.90	0.0950	0.50	10	4.31×10^{-10}	4.66×10^{-6}	3.26×10^{-4}
0.75	0.0222	0.25	5	4.69×10^{-7}	8.32×10^{-6}	2.17×10^{-4}
0.75	0.0222	0.25	10	2.48×10^{-12}	3.26×10^{-9}	2.12×10^{-7}
0.75	0.0558	0.50	5	1.39×10^{-5}	3.57×10^{-4}	1.04×10^{-2}
0.75	0.0558	0.50	10	2.34×10^{-9}	4.66×10^{-6}	3.26×10^{-4}
0.50	0.0031	0.25	5	1.38×10^{-6}	8.32×10^{-6}	2.17×10^{-4}
0.50	0.0031	0.25	10	3.93×10^{-11}	3.26×10^{-9}	2.12×10^{-7}
0.50	0.0123	0.50	5	3.98×10^{-5}	3.57×10^{-4}	1.04×10^{-2}
0.50	0.0123	0.50	10	3.62×10^{-8}	4.66×10^{-6}	3.26×10^{-4}

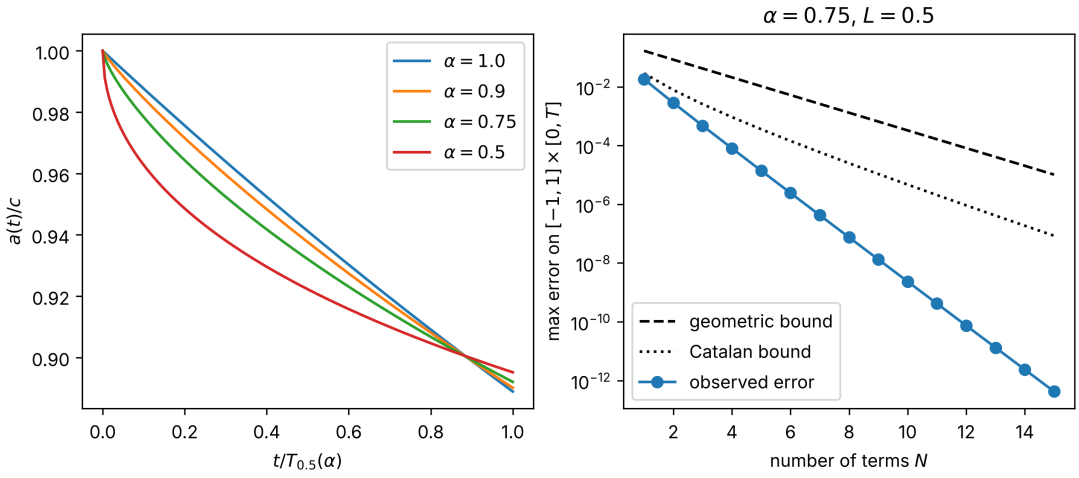


FIGURE 1. Linear initial data. Left: coefficient $a(t)/c$ up to the time at which $L = 1/2$. Right: observed error of ϕ_N and the bounds (4.5) for $\alpha = 0.75$.

For $\alpha < 1$, Table 3 lists the partial sums $\phi_N(1, 0.1)$. For $\alpha = 1$ they converge to the exact value 0.411001; for $\alpha < 1$ they first appear to settle and then grow without bound. Figure 4 shows the cause: the scaled coefficients $\|P_n\|_\infty/\Gamma(n\alpha+1)$ decrease geometrically for $\alpha = 1$ but grow super-geometrically for every $\alpha < 1$. This growth is not a rounding artefact: recomputing the coefficients in 80-bit extended precision changes them by less than 10^{-15} in relative terms.

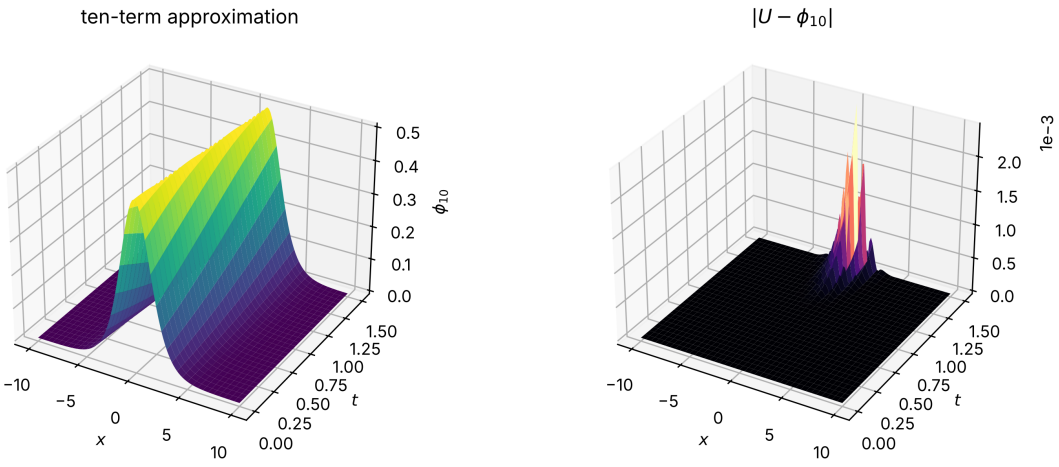


FIGURE 2. Soliton data, $\alpha = 1$: ten-term approximation ϕ_{10} (left) and its absolute error (right) on $[-10, 10] \times [0, 1.5]$.

TABLE 2. Soliton data, $\alpha = 1$: maximum error of ϕ_N on $[-20, 20] \times [0, T]$ and the bound (4.6).

T	N	observed	bound
0.5	5	2.10×10^{-4}	1.86×10^{-3}
0.5	10	4.51×10^{-8}	5.95×10^{-7}
0.5	15	6.36×10^{-12}	1.26×10^{-10}
1.0	5	6.46×10^{-3}	8.17×10^{-2}
1.0	10	4.51×10^{-5}	7.94×10^{-4}
1.0	15	2.00×10^{-7}	5.27×10^{-6}
2.0	5	1.82×10^{-1}	8.09×10^{0}
2.0	10	4.00×10^{-2}	1.99×10^{0}
2.0	15	5.75×10^{-3}	3.88×10^{-1}

TABLE 3. Soliton data: partial sums $\phi_N(x, t)$ at $x = 1$, $t = 0.1$.

α	$N = 3$	$N = 5$	$N = 8$	$N = 10$	$N = 15$
1.00	0.411042	0.411001	0.411001	0.411001	0.411001
0.90	0.416342	0.416226	0.41622	0.415477	−315.109
0.75	0.426703	0.426162	0.424801	−0.239914	-1.72×10^{7}
0.50	0.450999	0.443231	−1.52692	-1.23×10^{4}	-2.22×10^{14}

5.3. **Residual-based validation.** For fractional orders without a known exact solution, the accuracy of ϕ_N can be assessed through the fractional residual

$$R_N = {}^{C}D_t^{\alpha}\phi_N + 6\phi_N(\phi_N)_x + (\phi_N)_{xxx}, \tag{5.1}$$

which vanishes for the exact solution. By the second identity in (2.3), ${}^{C}D_t^{\alpha}u_n = t^{(n-1)\alpha}P_n/\Gamma((n-1)\alpha + 1)$ for $n \geq 1$, so R_N can be evaluated exactly from the polynomials P_n without numerical differentiation in time. Table 4 lists $\max|R_N|$

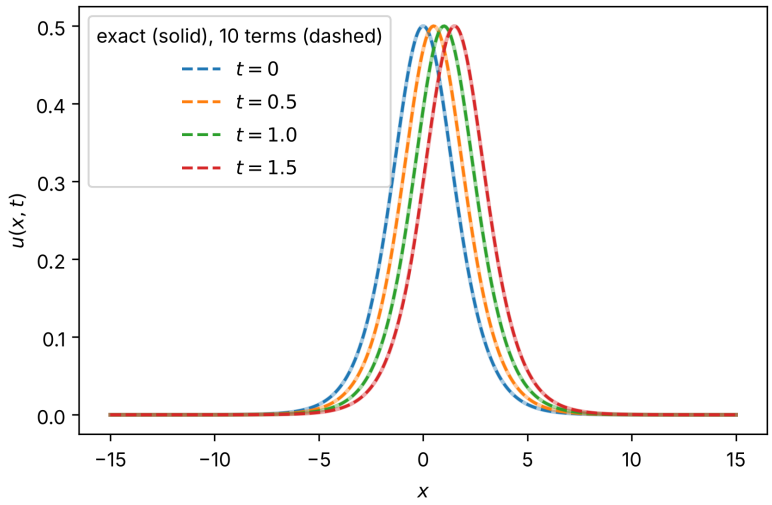


FIGURE 3. Soliton data, $\alpha = 1$: exact solution (solid) and ten-term Adomian–Elzaki approximation (dashed).

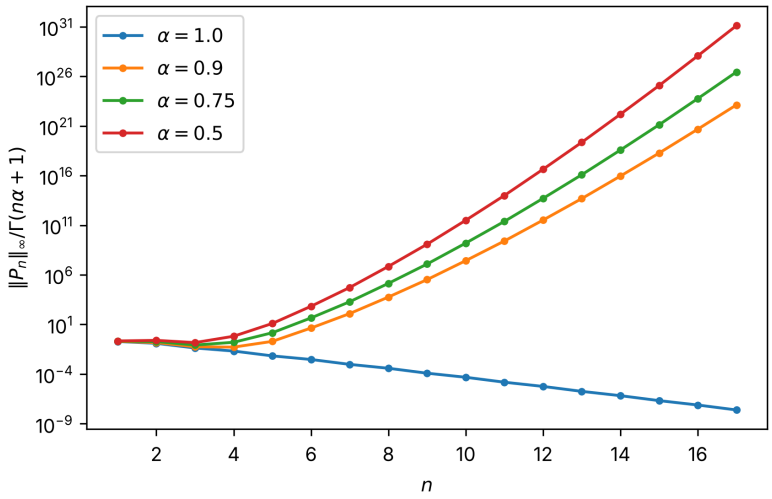


FIGURE 4. Soliton data: growth of the scaled coefficients $\|P_n\|_\infty/\Gamma(n\alpha + 1)$ of the Adomian–Elzaki series.

for linear data on $[-1, 1] \times [0, t]$, where t is the time at which $L = 1/2$; the residual decreases monotonically with N for every α, consistent with the convergence proved in Section 4. Table 5 lists $\max |R_N|$ for soliton data on $[-20, 20] \times (0, t]$. For $\alpha = 1$ the residual again decreases monotonically. For $\alpha < 1$ it decreases only up to a small number of terms and then grows rapidly; for $\alpha = 0.9$ and $t \leq 0.1$, for example, the smallest residual, 1.95×10^{-4}, is attained with $N = 5$ terms. This is the typical behaviour of a divergent asymptotic series, and it shows that the residual is a reliable practical criterion for choosing N: the series should be truncated where the residual stops decreasing.

TABLE 4. Linear initial data ($c = 1/6$, $\ell = 1$): maximum fractional residual $|R_N|$ on $[-1, 1] \times [0, t]$, with t such that $L = 1/2$.

α	$N = 3$	$N = 5$	$N = 8$	$N = 10$
1.00	7.20×10^{-3}	1.85×10^{-4}	5.73×10^{-7}	1.12×10^{-8}
0.75	8.46×10^{-3}	3.52×10^{-4}	2.63×10^{-6}	9.68×10^{-8}
0.50	9.86×10^{-3}	6.57×10^{-4}	1.17×10^{-5}	8.08×10^{-7}

TABLE 5. Soliton data: maximum fractional residual $|R_N|$ on $[-20, 20] \times (0, t]$.

α	t	$N = 3$	$N = 5$	$N = 8$	$N = 10$
1.00	0.1	1.37×10^{-3}	3.81×10^{-6}	3.46×10^{-10}	5.80×10^{-13}
1.00	0.5	4.43×10^{-2}	3.63×10^{-3}	5.80×10^{-5}	2.95×10^{-6}
0.90	0.1	2.49×10^{-3}	1.95×10^{-4}	1.72×10^{-2}	1.55×10^{0}
0.90	0.5	6.04×10^{-2}	6.84×10^{-2}	4.44×10^{2}	3.59×10^{7}
0.50	0.1	2.81×10^{-2}	2.13×10^{-1}	8.93×10^{3}	3.68×10^{10}
0.50	0.5	1.88×10^{-1}	5.42×10^{0}	4.23×10^{8}	7.19×10^{16}

5.4. **Arithmetic complexity.** For linear data each component is a scalar coefficient, and A_n requires $n+1$ products, so N terms cost $N(N-1)/2$ multiplications. For soliton data, P_n is a polynomial of degree $3n + 2$ in $\tanh(x/2)$, because each step applies three derivatives, each of which raises the degree by one. A product $P_j P'_{n-j}$ of polynomials of degrees $3j + 2$ and $3(n - j) + 3$ requires about $9j(n - j)$ multiplications, so A_n costs about $\sum_j 9j(n - j) \approx \frac{3}{2}n^3$, and N terms cost about $\frac{3}{8}N^4$ multiplications; the derivatives add only $O(N^2)$. If the components are instead stored on a grid of M points, A_n costs $O(nM)$ and N terms cost $O(N^2M + NM \log M)$. Table 6 and Figure 5 compare the counted multiplications with $3N^4/8$ and report the measured computing times (Python/NumPy, one core, best of five runs). The counts follow the N^4 law. The measured time grows more slowly, approximately like $N^{1.7}$ in this range, because the $O(N^2)$ calls to the vectorised polynomial product dominate for $N \le 40$; the N^4 term dominates only for larger N. For linear data, $N = 1000$ terms took 28 ms.

TABLE 6. Soliton data: degree of P_{N-1}, counted multiplications for generating N terms, the estimate $3N^4/8$, and measured computing time.

N	degree	multiplications	$3N^4/8$	time (ms)
5	14	375	234	0.61
10	29	4950	3750	2.30
15	44	23100	18984	5.02
20	59	69825	60000	6.40
30	89	337125	303750	13.94
40	119	1039350	960000	24.49

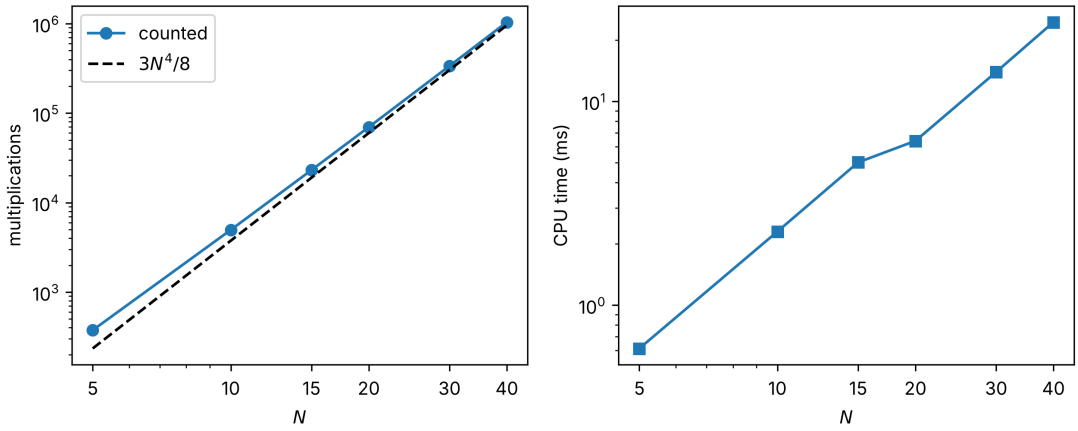


FIGURE 5. Soliton data: counted multiplications (left) and measured computing time (right) for generating N Adomian–Elzaki terms.

6. Discussion

The results of Sections 4 and 5 show that the behaviour of the Adomian–Elzaki method for the fractional KdV equation is determined by the interplay between the dispersive term u_{xxx} and the nonlinear term $6uu_x$. When the initial data belong to a class that is invariant under the iteration and on which u_{xxx} vanishes, as for linear data, the problem reduces to a fractional ordinary differential equation for the coefficient $a(t)$, the operator is a contraction for $T < T^*(\alpha)$, and the method converges with the explicit rate (4.5). The admissible horizon $T^*(\alpha)$ shrinks as α decreases, because $T^\alpha/\Gamma(\alpha+1)$ grows faster for small T when α is small; this reflects the stronger initial singularity of solutions of Caputo equations, which behave like $c + O(t^\alpha)$ near $t = 0$.

For soliton data the situation is different. At $\alpha = 1$ the series is the Taylor series of the travelling wave and converges up to the nearest complex singularity, at distance π. For $\alpha < 1$ the term proportional to $2 - \beta_2$ in (3.6) shows how the fractional coefficients break the cancellation between dispersion and nonlinearity, and the computations show that the resulting growth of the terms is faster than geometric. This is not a defect of the Elzaki transform, which only reorganises the computation of I_t^α, but a property of the formal series itself; Laplace-, Sumudu- or Shehu-based decomposition methods produce the same components and therefore the same behaviour. In practice, truncated Adomian–Elzaki series for dispersive fractional equations should be interpreted as asymptotic approximations for small t, with the number of terms chosen by monitoring the residual (5.1); when accuracy over longer times is required, time-stepping schemes such as the predictor–corrector method of [5] are more appropriate.

The complexity analysis of Section 5 complements this picture. Generating N terms symbolically costs about $\frac{3}{8}N^4$ multiplications for soliton data because the polynomial degree grows linearly with N, whereas for linear data the cost is only quadratic. For data with growing complexity, a fixed spatial grid with M points

reduces the cost to $O(N^2M)$, but it does not change the convergence properties discussed above.

7. Conclusion

The convergence of the Adomian–Elzaki method for the time-fractional KdV equation depends essentially on the initial data. For data linear in space, the method is a strict contraction on an explicit Banach space with constant $L = 24cT^\alpha/\Gamma(\alpha+1)$, and the Adomian terms obey a Catalan-number bound that gives a computable a priori error estimate, confirmed by the computations. For soliton data, the series converges for $t < \pi$ when $\alpha = 1$, whereas for $\alpha < 1$ the loss of the cancellation present in the integer-order case leads to divergence. Convergence claims for transform–decomposition methods applied to dispersive fractional equations should therefore be supported by problem-specific estimates of the kind given here. Extending the contraction analysis to other invariant classes of data and developing summation techniques for the divergent case are natural directions for further work.

Acknowledgement. The authors thank the editor and the anonymous reviewer for their careful reading and constructive comments, which substantially improved this paper.

References

[1] Adomian, G. (1994). *Solving frontier problems of physics: The decomposition method* (Fundamental Theories of Physics, Vol. 60). Springer. https://doi.org/10.1007/978-94-015-8289-6

[2] Caputo, M. (1967). Linear models of dissipation whose Q is almost frequency independent–II. *Geophysical Journal International*, 13(5), 529–539. https://doi.org/10.1111/j.1365-246X.1967.tb02303.x

[3] Cherruault, Y. (1989). Convergence of Adomian's method. *Kybernetes*, 18(2), 31–38. https://doi.org/10.1108/eb005812

[4] Diethelm, K. (2010). *The analysis of fractional differential equations* (Lecture Notes in Mathematics, Vol. 2004). Springer. https://doi.org/10.1007/978-3-642-14574-2

[5] Diethelm, K., Ford, N. J., & Freed, A. D. (2002). A predictor-corrector approach for the numerical solution of fractional differential equations. *Nonlinear Dynamics*, 29, 3–22. https://doi.org/10.1023/A:1016592219341

[6] Elzaki, T. M. (2011). The new integral transform "Elzaki transform". *Global Journal of Pure and Applied Mathematics*, 7(1), 57–64.

[7] He, W., Chen, N., Dassios, I., Shah, N. A., & Chung, J. D. (2021). Fractional system of Korteweg–de Vries equations via Elzaki transform. *Mathematics*, 9(6), 673. https://doi.org/10.3390/math9060673

[8] Korteweg, D. J., & de Vries, G. (1895). On the change of form of long waves advancing in a rectangular canal, and on a new type of long stationary waves. *The London, Edinburgh, and Dublin Philosophical Magazine and Journal of Science*, 39(240), 422–443. https://doi.org/10.1080/14786449508620739

[9] Lutz, D. A., Miyake, M., & Schäfke, R. (1999). On the Borel summability of divergent solutions of the heat equation. *Nagoya Mathematical Journal*, 154, 1–29. https://doi.org/10.1017/S0027763000025289

[10] Momani, S. (2005). An explicit and numerical solutions of the fractional KdV equation. *Mathematics and Computers in Simulation*, 70(2), 110–118. https://doi.org/10.1016/j.matcom.2005.05.001

[11] Nafia, E.-M., Alatoune, H., & El Omari, M. (2026). Devaney chaos of a proportional Caputo derivative. *Annals of Mathematics and Computer Science*, 36. https://doi.org/10.56947/amcs.v36.940

[12] Oyefusi, A. S., Odetunde, O. S., Onitilo, S. A., & Adepoju, J. T. (2026). Operator theoretic analysis of coupled decomposition methods. *Annals of Mathematics and Computer Science*, 36. https://doi.org/10.56947/amcs.v36.926

[13] Zair, K., Oufkir, K., & Elomari, M. (2026). Fractional Burgers equations with mixed derivatives. *Annals of Mathematics and Computer Science*, 36. https://doi.org/10.56947/amcs.v36.949

[1] Department of Mathematics, SNJB's KKHA Arts, SMGL Commerce and SPHJ Science College, Chandwad, Nashik, Maharashtra, India.

Email address: m16zanje@gmail.com

[2] Department of Mathematics, Rani Laxmibai Mahavidyalaya, Parola, Jalgaon, Maharashtra, India.

Email address: saisns@rediffmail.com